International Journal of Plastics Technology (June 2019) 23(1):110–121
https://doi.org/10.1007/s12588-019-09237-4

RESEARCH ARTICLE

Poly(acrylic acid-*co*-styrene)/clay nanocomposites: efficient adsorbent for methylene blue dye pollutant

Zoulikha Djamaa[1,2] · Djahida Lerari[1,3] · Abderrezak Mesli[2] · Khaldoun Bachari[1]

Received: 13 February 2019 / Accepted: 23 March 2019 / Published online: 23 April 2019

Abstract
In this contribution, polymer/clay (nano)composites, based on poly(acrylic acid) (PAA) and poly(acrylic acid-*co*-styrene) poly(AA-*co*-St), were synthesized by free radical polymerization, using 2,2′-azobis(isobutyronitrile) (AIBN), as initiator and organomodified clay (OMMT), as nanofillers. The structural and morphological characteristics of the obtained (nano) composites, PAA/OMMT (1, 3, 5 wt%), poly(AA_{75}-*co*-St_{25})/OMMT (3 wt%) and poly(AA_{25}-*co*-St_{75})/OMMT (3 wt%), were examined by X-ray diffraction and scanning electron microscopy, indicating the successful intercalation of polymer chains into the clay nanoplatelets. Thermal properties of obtained (nano)composites were evaluated according to thermogravimetric analysis and differential scanning calorimetry. Based on morphological and thermal results, poly(AA_{25}-*co*-St_{75})/OMMT (3 wt%) (nano)composite was selected as an efficient adsorbent matrix for methylene blue dye, with about 74% of elimination obtained after only 80 min of swelling, under soft conditions.

Keywords Nanocomposites · Poly(acrylic acid-*co*-styrene) · Montmorillonite · Adsorption

Introduction

The incorporation of fillers in polymers is known as one of the techniques allowing to improve the properties of the materials and to expand their application fields. Moreover, it is an economic way to develop new materials with enhanced properties (mechanical proprieties, thermal stability, flame retardancy, optical properties and permeability) for different specific applications [1–7]. It is clear that different materials were employed as nanofillers in polymers matrix, such as clays, carbon nanotube, nanowires or colloidal silica [8–10]. However, lamellar clays are one of the most used, because of its existence as an abundant natural resource. However, it is the surface nanoplatelet must be organomodified in order to reduce the hydrophilic character of the clay and hence, improve their dispersion in hydrophobic polymer matrix [11–14]. So, depending on the clay class and chemical structure of the polymer, several methods have been employed leading to polymer/clay nanocomposites with improved physicochemical properties, especially, melt intercalation [15, 16], template synthesis [17], exfoliation adsorption [18], and in situ polymerization [19–22]. In the case of acid acrylic monomer, many studies were established regarding the preparation of nanocomposites with improved properties [1, 23–25]. Recently, Luecha and Magaraphan [1] reported the results regarding the enhancement of thermal and mechanical properties of poly(acrylic acid) gel reinforced polyethylene terephthalate/clay nanocomposite. On the other hand, Supri et al. [23] examined the poly(acrylic acid) effect on morphology and mechanical properties of LDPE/clay composites. Also, Bo et al. analyzed the structure and morphology of poly(acrylic acid)-based kaolin (nano)composites prepared by in situ polymerization, and Liu et al. studied the adsorption proprieties of cross-linked poly(acrylic acid)/clay (nano)composites prepared using redox initiator [24, 25]. Similar studies were established regarding polystyrene (nano)composites for improving the thermal and

✉ Djahida Lerari
lerari_zinai@yahoo.fr

[1] Centre de Recherche Scientifique et Technique en Analyses Physico-chimiques, BP 384, Zone Industrielle Bou-Ismail, RP 42004 Tipaza, Algeria

[2] Laboratoire de Chimie Organique Physique et Macromoléculaire (LCOPM), Université de Sidi Bel-Abbès, Département de Chimie, BP 89, 22000 Sidi Bel-Abbès, Algeria

[3] Laboratoire de Synthèse Macromoléculaire et Thio-organique Macromoléculaire, Faculté de Chimie, Université des Sciences et de la Technologie Houari Boumediene, BP 32, El-Alia, 16111 Bab-Ezzouar, Alger, Algeria

mechanical properties as well as the oxygen diffusion and flammability [26–29]. The combination of poly(acrylic acid) and polystyrene using different methods, such as: emulsion, radical polymerization, controlled polymerizations was also reported in the literature [30–33]. However, the use of the copolymer for the adsorption of some organic molecules proved to be one of the more important application ways which interests the researchers. Recently, El-Segeny et al. synthesized the hybrid styrene/acrylic acid/clay by irradiation and tested the sorption of the acid green B and maxilon C.I. basic dyes molecules, respectively. The amount of adsorbed dyes achieved about 58 mg/g and 78 mg/g, after 12 h for acid green B and maxilon C.I. basic, respectively [34]. Wang et al. [35] and Bulut et al. [36] studied the adsorption of methylene blue (MB) dye using the chitosan-g-PAA/clay (nano)composites. It is known that methylene blue (MB) is one of the most commonly used materials for dying cotton and textiles. Consequently, it is largely present in water industrial rejects. Furthermore, it can cause permanent injury for health. Combining the physicochemical properties of poly(acrylic acid) and polystyrene matrixes as well as that of natural Algerian clay for producing material (nano) composites, to remove methylene blue (MB) dye is the aim of this contribution. However, remarkable increase in nanoplatelets distance accompanied with improved thermal and mechanical properties of poly(methyl methacrylate)/clay (nano)composites was noticed in presence of this clay, used as nanofiller [11, 20, 37]. Furthermore, many studies are discussed the application of this natural clay [38–40]. In this work, poly(acrylic acid-*co*-styrene)/clay (nano)composites were synthesized by in situ radical polymerization. Clay (MMT) has been first organically modified with hexadecyl trimethyl ammonium bromide (HDTMA) to produce a modified nanoclay (OMMT). The morphology and thermal properties of the resulting (nano)composites have been investigated by X-ray diffraction (XRD), scanning electron microscopy (SEM), thermogravimetric analysis (TGA) and differential scanning calorimetry (DSC). The efficiency of the material, as adsorbent matrix of the MB dye, was evaluated under easy experimental conditions.

Experimental part

Materials

The monomers acrylic acid (AA) and styrene (St) (Aldrich Chemical, 98%) were distilled under reduced pressure prior to use. The free radical initiator, 2,2′-azobis(isobutyronitrile) (AIBN) (Aldrich, 98%) was purified by recrystallization in methanol. Hexadecyl trimethyl ammonium bromide (HDTMA) (Aldrich, 99%) was used without further purification. Toluene and heptane were provided from Aldrich Chemical and used after distillation. The Algerian clay (MMT) used in this study was natural montmorillonite from Mostaganem (Algeria), kindly supplied by Entreprise Nationale des Produits Miniers Non-Ferreux et des Substances Utiles (ENOF), Algeria. MMT chemical composition $(Si_{4.24})^{IV}(Al_{1.24}\ Mg_{0.2}\ Fe_{0.17}\ Ti_{0.01})^{VI}\ O_{10}\ (OH)_2$, nH_2O $Na_{0.13}$, $Ca_{0.01}$, $K_{0.1}$ was determined by the supplier. The dye used in the experiments was methylene blue (MB) (Cheminova International). It was used without further purification.

Organomodification of the clay (OMMT)

Firstly, the natural clay was dispersed in aqueous solution, and the organic impurities were eliminated by treatment with hydrogen peroxide. Then, montmorillonite (MMT) was converted into its sodic from by treatment with NaCl. Finally, the organophilic form of MMT was obtained by ion-exchange reaction of the Na^+ cations with HDTMA molecules, as reported elsewhere [11]. Briefly, to a suspension of sodic montmorillonite was added the ammonium bromide freshly dispersed in distilled water. After one night at 80 °C under mechanical stirring, the mixture was filtered off and the collected organomodified clay was washed with hot water to eliminate excess ammonium bromide (as checked by $AgNO_3$ test) and sodium ions. The organomodified clay was then freeze-dried for about 12 h. The obtained organophilic montmorillonite is noted as OMMT.

Synthesis of poly(acrylic acid)/clay (nano) composites (PAA/OMMT)

Different amounts of organomodified clay OMMT (1, 3, and 5 wt%) were stirred for 24 h in toluene. Then, acrylic acid monomer, AIBN (0.1 wt%), were introduced under nitrogen flow in the reactor, and the polymerization was carried out at 70 °C for 1 h under nitrogen. Finally, the polymer was collected by precipitation in heptane dried at room temperature and then in vacuum oven. For the sake of comparison, unifilled polymer poly(acrylic acid) (PAA) was synthesized under the same conditions.

Synthesis of poly(acrylic acid-*co*-styrene) (nano) composites (poly(AA-*co*-St)/OMMT)

Freshly distilled acrylic acid and styrene monomers, AIBN (0.1 wt%) as free radical initiator and organomodified clay OMMT (3 wt%), in toluene, were placed in the reactor and stirred at room temperature under nitrogen flow for few minutes for homogenization. The temperature was increased at 70 °C, and the polymerization was carried out for 8 h. The obtained (nano)composites noted poly(AA_{75}-*co*-St_{25})/OMMT and poly(AA_{25}-*co*-St_{75})/OMMT was collected by

precipitation in heptane, dried at room temperature and then in vacuum oven.

Determination of isoelectric point (PZC) of adsorbent

The isoelectric point (PZC) of an adsorbent is an important parameter to characterize the solid–solution interface. It is defined as the point in which, adsorbent possess a null charge potential on its surface. In order to determine the PZC of poly(AA_{25}-*co*-St_{75})/OMMT, used as adsorbent, different solutions with different initial pH values (pH_i = [2–12]) were prepared by addition of 0.1 M aqueous solution of HCl or NaOH and then mixed at room temperature for few minutes. After 48 h, the pH of each solution was measured (noted pH_f). The PZC is identified as the point at which the change of pH is equal to 0 [40].

Adsorption of MB dye on nanocomposite surface

The adsorption experiments were performed according to the following method: 50 mg of poly(AA_{25}-*co*-St_{75})/OMMT, as adsorbent was added to a MB solution at a concentration of 50 mg/L and 100 mg/L, respectively. The solution was stirred at room temperature. The stirring time was selected in the interval [0–120 min]. Then, the poly(AA_{25}-*co*-St_{75})/OMMT was separated by filtration and the residual concentration of MB in solution was determined by UV–Vis spectrophotometry. The amount of adsorbed dye (mg/g) was calculated using the following equation (Eq. 1):

$$q_e = \frac{(C_i - C_f)V}{m} \quad (1)$$

where q_e is the amount of dyes adsorbed onto dry mass of the poly(AA_{25}-*co*-St_{75})/OMMT (nano)composite (mg/g), C_i and C_f are the concentrations (mg/L) of the dye solution before and after adsorption, respectively. V is the volume of the aqueous phase (L), and m is the weight of dry adsorbent (g). The percent of adsorbed MB on the adsorbent matrix [R (%)] was calculated according to Eq. 2.

$$R\% = \frac{C_i - C_f}{C_i} \times 100. \quad (2)$$

Instrumentation

Fourier transform infrared (FTIR) spectra of obtained (nano) composites were recorded on the transmission mode using Fourier transform (ALPHA) of BRUKER spectrophotometer at 2 cm^{-1} resolution with 32 scans over the spectral range of 4000–400 cm^{-1}. X-ray diffraction (XRD) patterns were performed using Siemens D5000 diffractometer, using monochromatic CuKα radiation ($\lambda = 0.15406$ nm) from 1.65° to 30° by step of 0.04° and scanning rate of 10°/min. Scanning electron microscopy (SEM) images of the systems were obtained, using Quanta 250 instrument equipped with a field emission filament using an acceleration voltage of 5 kV and a working distance of 10 mm. Thermal properties of (nano) composites were evaluated by using thermogravimetry analysis (TGA). Measurements were carried out by thermal analysis calorimeter SDT Q600, from ambient to 600 °C, at a heating rate of 10 K min^{-1}, in a nitrogen atmosphere at flow rate of 20 ml min^{-1}. The glass transition temperatures (T_g) of the synthesized materials were determined by differential scanning calorimetry (DSC) using a calorimeter SDT Q600. The adsorption of methylene blue was evaluated by ultraviolet (UV–visible) spectrophotometer Optizen 1420 V, using a Shimadzu UV-160. Quartz cell of 1 cm path length was used in the analysis.

Results and discussion

Structure and morphology

Figure 1 shows FTIR spectra of synthesized PAA/OMMT (nano)composites. The bands appeared in 1401–1438 cm^{-1} region and at 1703 cm^{-1}, result from the bending vibrations of $–CH_2$ and –C=O groups of PAA polymer, respectively. Furthermore, additional peaks, assigned to the modified clay, were detected, which confirm the presence of nanofiller in the polymer matrix. In particular, the peak around 1021 cm^{-1} and 470 cm^{-1} resulted from the stretching and bending vibrations of Si–O, respectively [24]. The peak at 458 cm^{-1} is assigned to Mg-O bond in OMMT. In the case of poly(AA-*co*-St), the characteristic bands of styrene were noticed (Fig. 2). The stretching vibrations of phenyl groups were detected at 702 cm^{-1}, 751 cm^{-1} and 1447 cm^{-1}. The characteristic stretching band of carbonyl groups is observed at 1708 cm^{-1}. The evaluation of dispersion degree of the OMMT in the polymers-based (nano)composites was established according to the X-ray diffraction (XRD), using the Bragg's equation n $\lambda = 2d \sin\theta$ (n is an integer determined by the order given, λ is the wavelength of X-rays, d is the spacing between the planes in the atomic lattice, and θ the angle between the incident ray and the scattering planes). As shown in Fig. 3a, defined diffraction peak of the modified clay (OMMT) is appeared at $2\Theta = 3.95°$, with an interlamellar distance of 23.67 Å. As far as the nanocomposites PAA/OMMT (1, 3, 5 wt%) are concerned, the XRD patterns display large diffraction peaks ranging between 1.25 and 2.5 Å. In this case, it is difficult to conclude the structure of the synthesized PAA-based (nano)composites, but it is clear to claim the absence of exfoliation structure [1]. Interestingly, defined XRD peaks centered around $2\Theta = 1.98°$ were detected with poly(AA-*co*-St)/OMMT-based (nano)

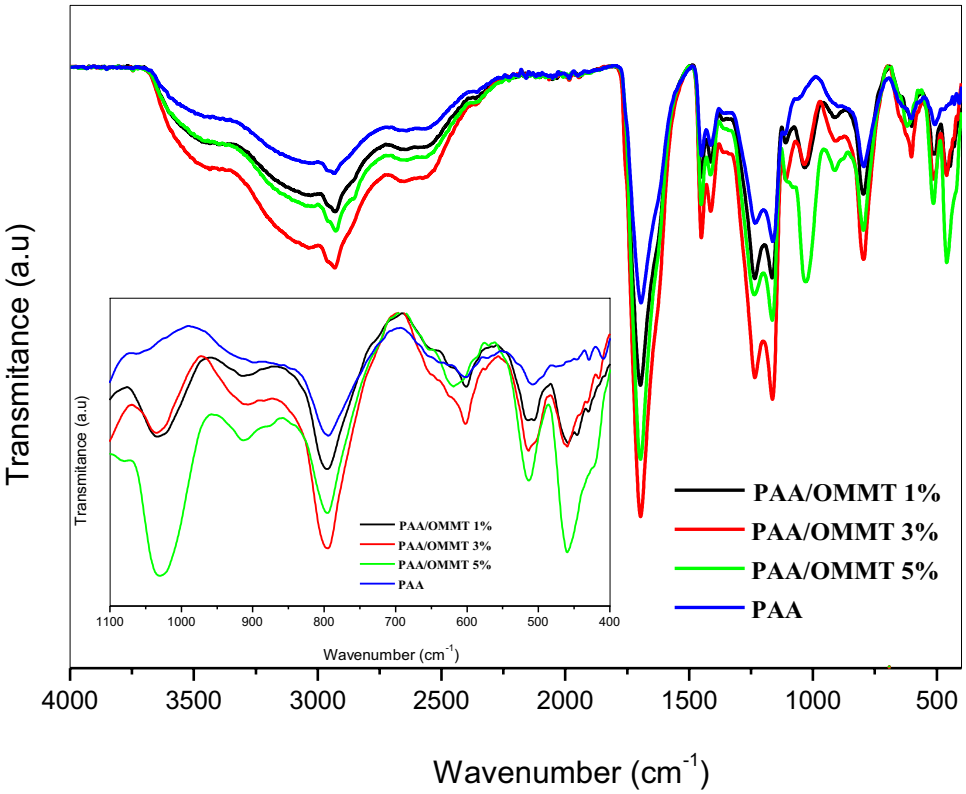

Fig. 1 FTIR spectra of PAA and PAA/OMMT (nano)composites

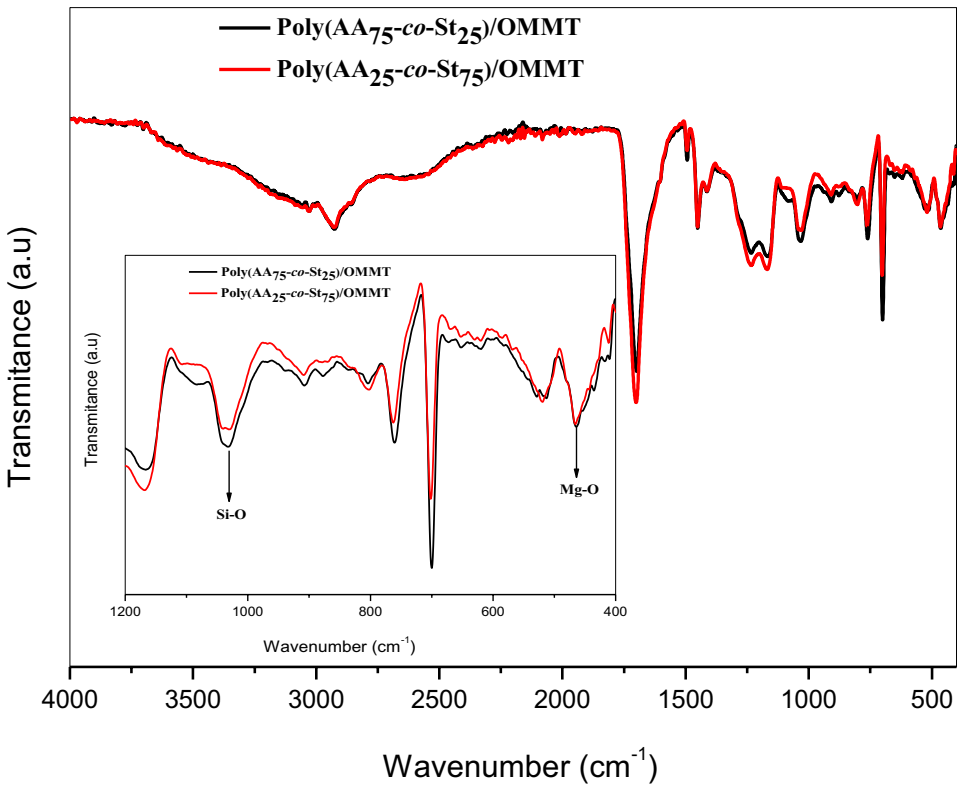

Fig. 2 FTIR spectra of poly(AA_{75}-*co*-St_{25}) and poly(AA_{25}-*co*-St_{75})/OMMT (nano)composites, at 3 wt% of clay

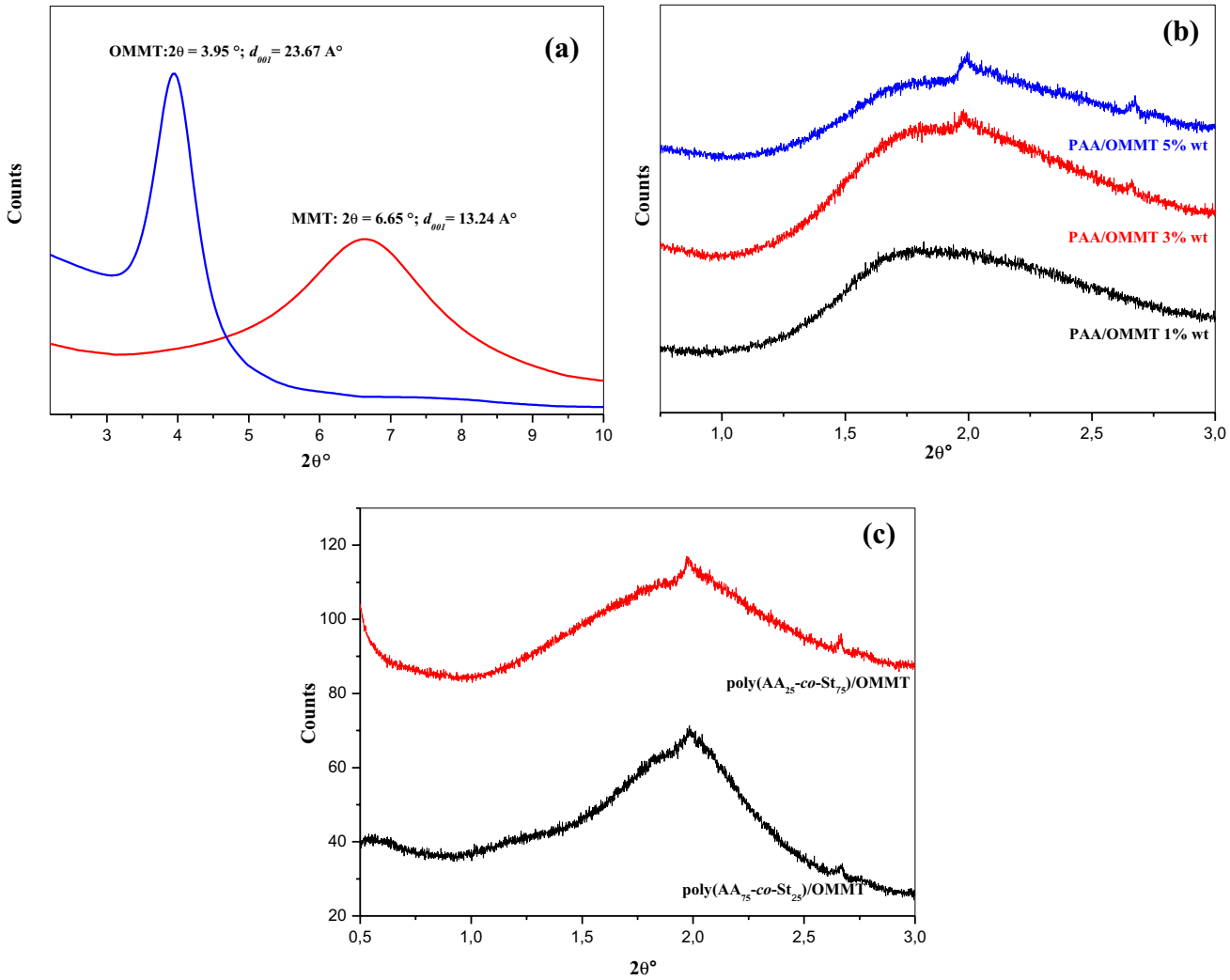

Fig. 3 XRD patterns of clay before and after organomodification (**a**), poly(acrylic acid)/OMMT-based (nano)composites, at different organomodified clay contents (**b**) and poly(acrylic acid-*co*-styrene)/OMMT-based (nano)composites containing 3 wt% of organomodified clay (**c**)

composites, whatever the co-monomer styrene content (Fig. 3c). This important shift of the 001 plane peak of clay in presence of polymer matrix attests for some level of clay delamination ($2\Theta = 1.98°$, $d_{001} = 44.8$ Å). Complementary information regarding the morphology of these systems is obtained by SEM. The images recorded over thin slides fully attest a difference in the surface by adding nanoclay. As shown in Fig. 4a, the PAA polymer presents a clear surface. Rather, the organomodified clay enables some modification in the polymer matrix surface by the appearance of some imperfection, as observed from SEM images of Fig. 4b. Indeed, no trace of micrometer-sized clay agglomerates is detected. A different surface morphology can be clearly observed in the case of poly(AA-*co*-St)/OMMT (nano)composites. Some clay sheet superposition resulting from their dispersion in the polymer matrix is evidenced by the MEB images illustrated in Fig. 4c. Such difference might be explained by the presence of styrene *co*-monomer which improves the clay nanoplatelets disaggregation. This result agrees with the increase in the interlamellar distance, as obtained by DRX analysis. In conclusion, intercalated (nano)composites structure was obtained with poly(AA-*co*-St) copolymer whatever the co-monomer fraction in the matrix. This result is more likely attributed to the shift of the interlayer spacing clay triggered by the ammoniums cations. This shift is furthermore accentuated in the presence of copolymer chains that significantly separate the clay nanoplatelets.

Thermal properties

Figures 5 and 6 show the TGA and DTG curves of virgin poly(acylic acid), poly(acrylic acid-*co*-styrene) and their corresponding (nano)composites, as recorded under nitrogen

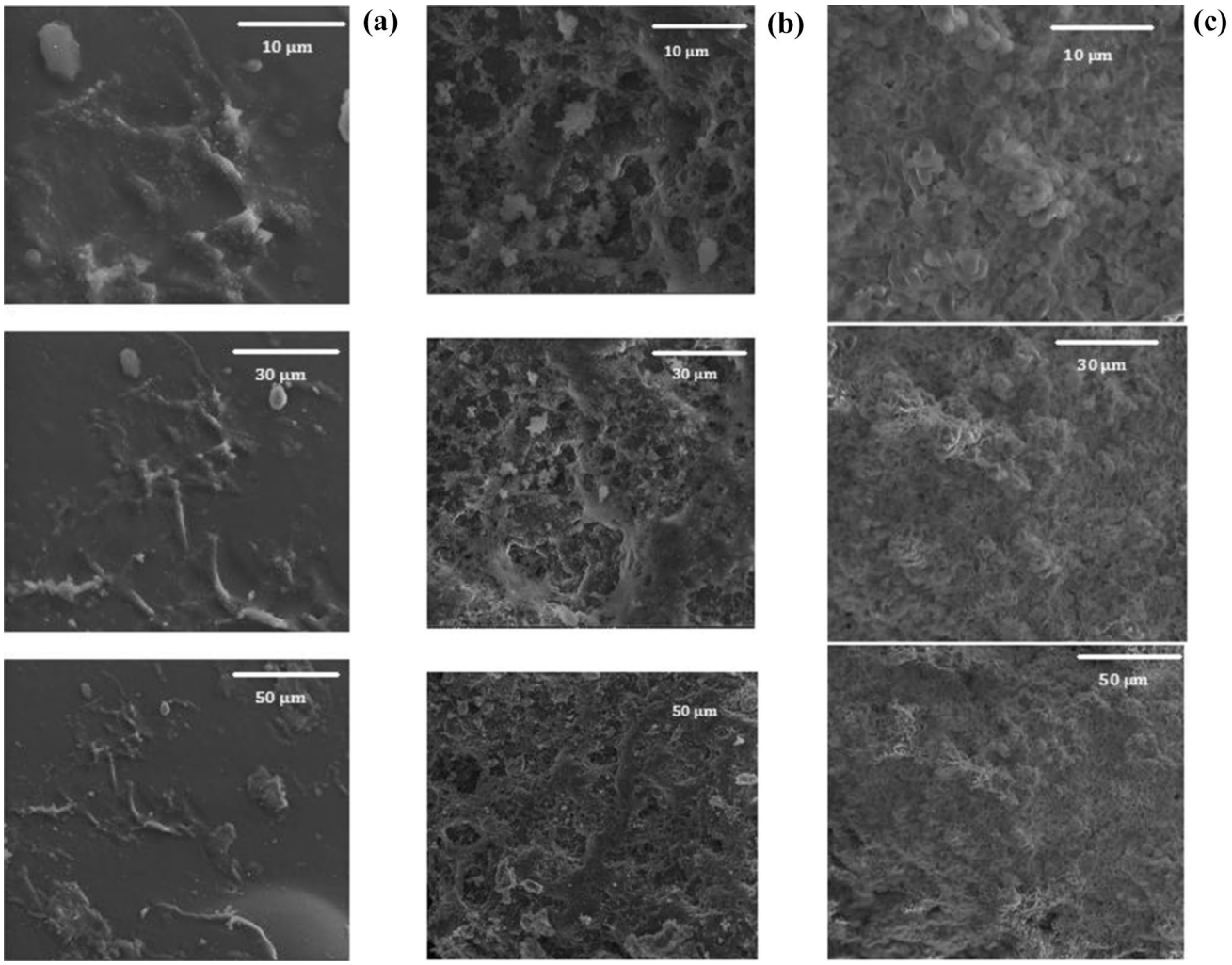

Fig. 4 SEM micrographs for **a** PAA, **b** PAA/OMMT and **c** poly(AA_{25}-*co*-St_{75})/OMMT (nano)composites, at 3 wt% of clay

flow. As shown in Fig. 5, poly(acrylic acid) displays three degradation steps with a maximum degradation at 132 °C, 310 °C and 421 °C, respectively. The first peak of degradation becomes less apparent when the nanoclay was dispersed in the PAA matrix. On other words, the start degradation of the PAA/OMMT (nano)composites is shifted to higher temperature, where the DTG curve regroup the first and the second steps of degradation. Thermo-degradation of poly(AA_{25}-*co*-St_{75})-based (nano)composites was also carried out. TGA and DTG curves are demonstrated in Fig. 6. The shape of the DTG curves is clearly different from that of the PAA matrix, in which three degradation steps are noticed, with a first DTG peak around 132 °C. Interestingly, the degradation behavior of poly(AA_{25}-*co*-St_{75})/OMMT and poly(AA_{75}-*co*-St_{25})/OMMT (nano)composites is occurred in one step, with the absence of the first and second degradation steps. However, poly(AA_{25}-*co*-St_{75})/OMMT (nano)composite shows a remarkable thermal stability, with a maximum degradation temperature located at 421 versus 403 °C for poly(AA_{75}-*co*-St_{25})/OMMT(nano) composite. Consequently, the homogenous dispersion of the nanofiller in the copolymer matrix shows a significant delay in weight loss. The organoclay nanoplatelets act as physical barriers that are able to refrain the diffusion of the heat flow to the polymer matrix. This effect is in agreement with the morphology of the poly(AA_{25}-*co*-St_{75})/OMMT and poly(AA_{75}-*co*-St_{25})/OMMT (nano)composites, in which the clay sheet are homogeneously dispersed, as evidenced by SEM analysis. The effect of OMMT on T_g of the synthesized polymers (nano)composites was also examined using DSC (Table 1). The T_g values of PAA remain not affected by the presence of the nanofiller. Any remarkable increase in the T_g value was noticed (Fig. 7a). However, the confinement of the polymer chains is affected by the presence of styrene co-monomer, to underline an increase in the T_g (Fig. 7b) [11, 26]. It can be concluded that the poly(AA_{25}-*co*-St_{75})/OMMT (nano)composite displays better structure than the other systems. It exhibits homogenous morphology accompanied by

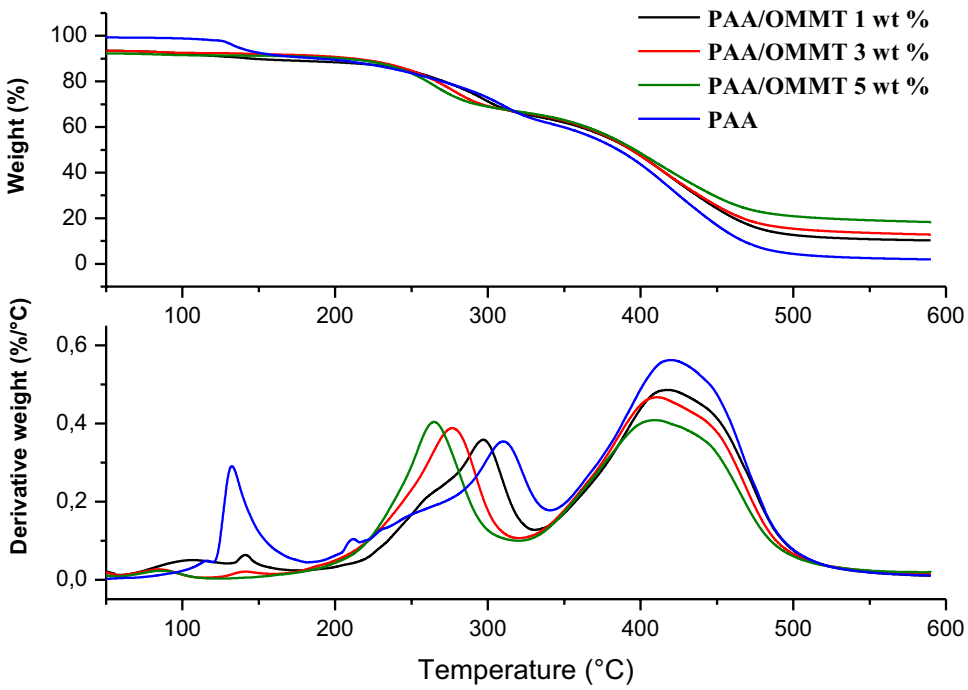

Fig. 5 Thermogravimetric analysis curves of PAA and PAA/OMMT with different percents of inorganics, at 20 °C/min

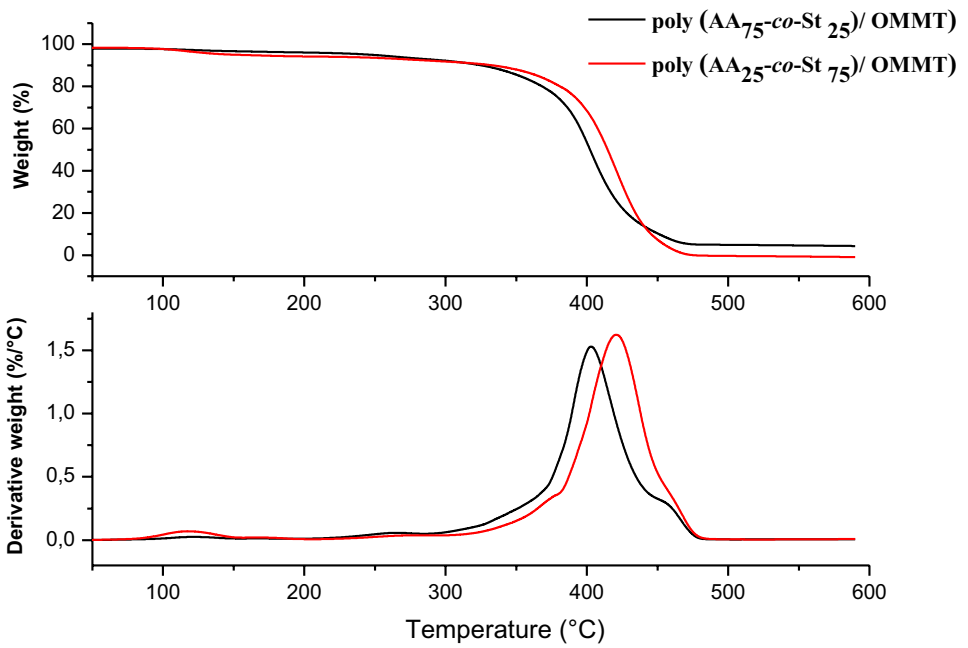

Fig. 6 Thermogravimetric analysis curves of poly(AA-*co*-St)/OMMT-based (nano)composites with 3 wt% of inorganics, at 20 °C/min

remarkable thermal stability below 300 °C. For this, it was selected, in this study, as a material for adsorption of methylene blue (MB), considered as pollutant.

Isoelectric point (PZC) of poly(AA_{25}-*co*-St_{75})/OMMT

According to the curve illustrated in Fig. 8, it is noticed that the zeta potential values are positives at pH < 3.6, and then the (nano)composite is positively charged. Although, at pH > 3.6, the (nano)composite is negatively charged. Hence, the isoelectric point (PZC) of poly(AA_{25}-*co*-St_{75})/OMMT is equal to 3.6.

Table 1 Thermogravimetric parameters of PAA, poly(AA-*co*-St) and their (nano) composites

System	Nanofiller content (wt%)	T_{10} (°C)	T_{50} (°C)	T_d max (°C)	T_g (°C)
PAA/OMMT	0	148	324	416	92
	1	229	305	418	128
	3	234	308	412	134
	5	230	305	409	132
P(AA-*co*-St)	0	233	406	412	155
Poly(AA_{25}-*co*-St_{75})/OMMT	3	316	401	401	161
Poly(AA_{75}-*co*-St_{25})/OMMT	3	316	413	409	162

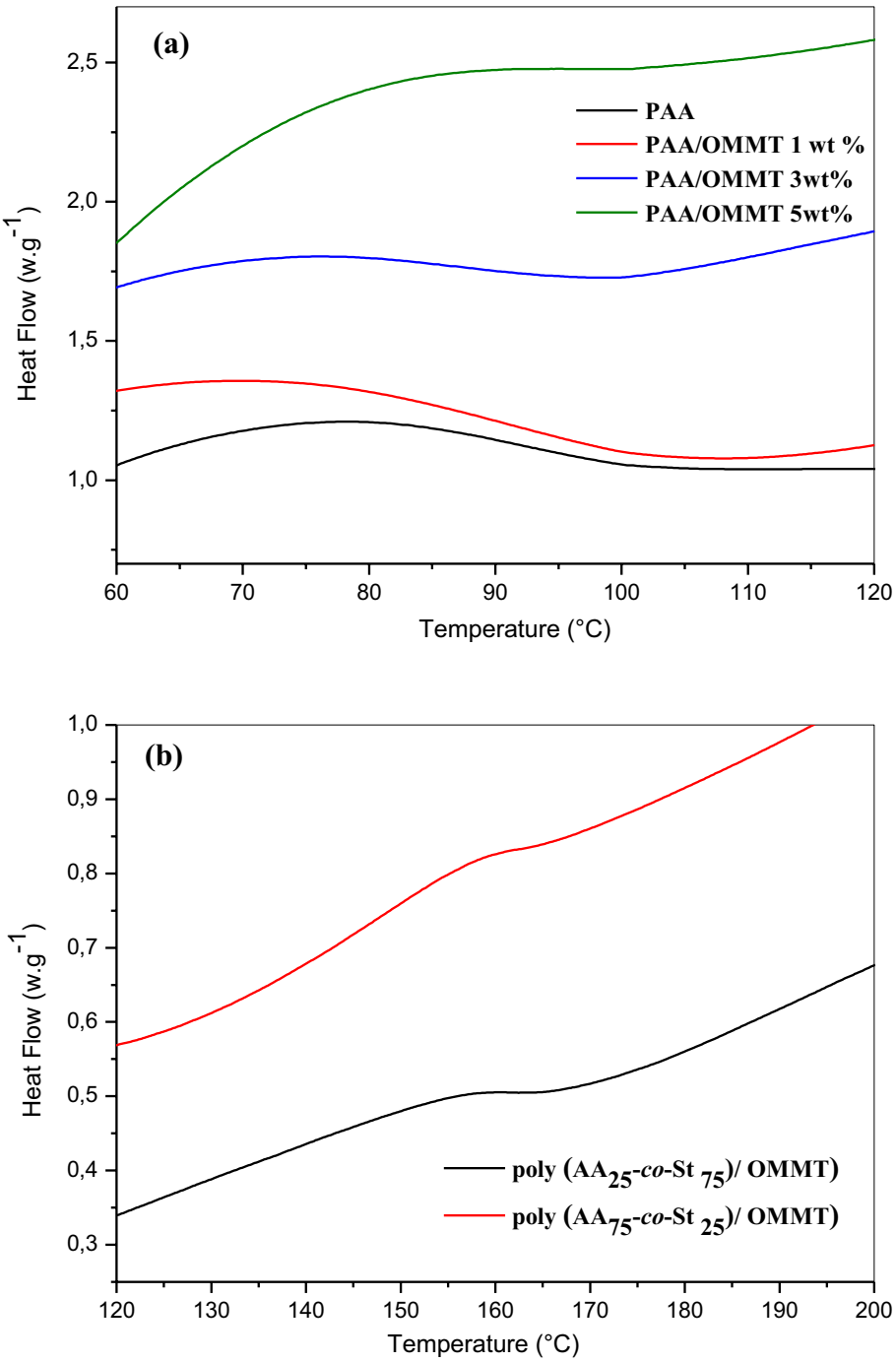

Fig. 7 DSC scans (second run) for **a** PAA/OMMT-based (nano)composites with different percents of inorganics and **b** poly(AA-*co*-St)/OMMT-based (nano)composites with 3 wt% of inorganics

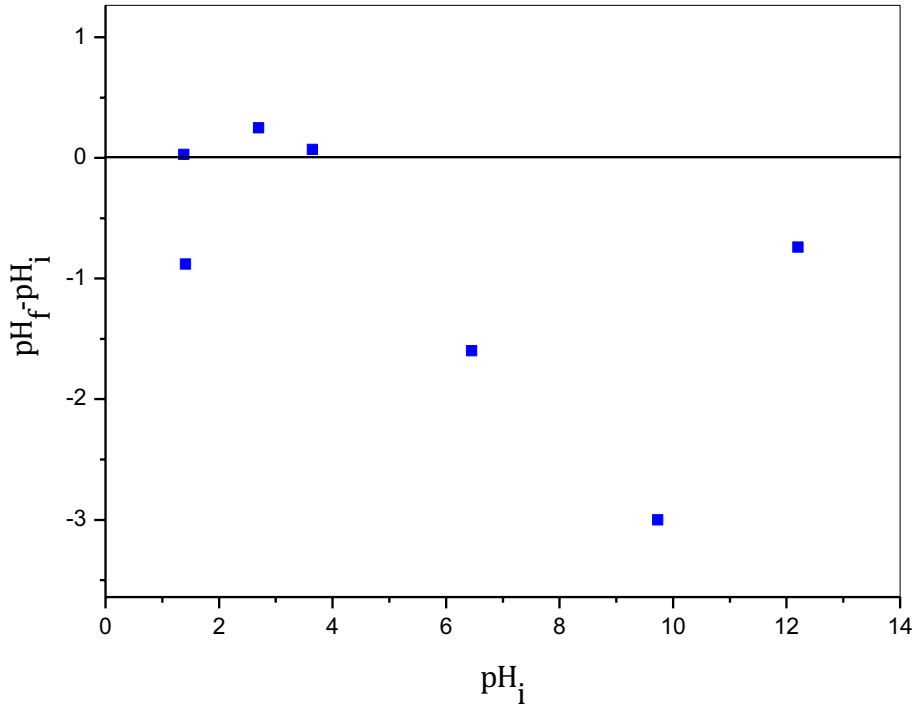

Fig. 8 Isoelectric point of poly(AA_{25}-*co*-St_{75})/OMMT 3 wt%

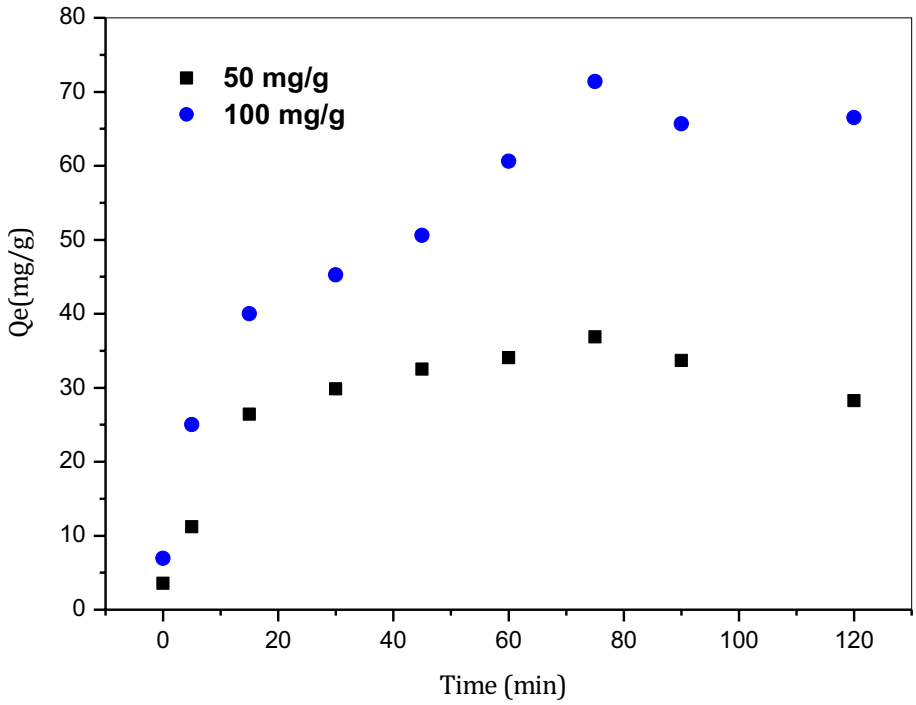

Fig. 9 Evolution of the blue methylene (MB) adsorption versus time

Adsorption of methylene blue (MB)

Figure 9 shows the dependence of MB adsorption on time, in which the MB adsorption increased by increasing the time contact whatever the initial concentration of dye. However, a remarkable adsorption percent was observed in the few minutes of stirring, due to the greater availability of vacant sites of adsorbent surface, with an adsorbed amount of about 26 mg/g and 40 mg/g for an initial concentration of 50 mg/L and 100 mg/L, respectively, which correspond to about 52% and 40% of removal. After 30 min of stirring, a partial saturation of available sites was achieved. So, the remaining vacant external sites become difficult to occupy because of the formation of repulsive forces between the dye molecules existing on the adsorbent surface and those on the aqueous phase. Furthermore, there is such diffusion of MB molecules in the interlamellar spaces of nanofiller until they are saturated, which will reduce the mass transfer between the liquid phase and the solid phase with time, whereby the removal percentage became constant, reaching a maximum values of about 74% and 72% for an initial concentration of 50 mg/L and 100 mg/L, respectively. Thus, a stirring time of 75 min can be considered as the time where the balance of the adsorption of MB is achieved. Hence, it is concluded that the studied (nano)composite shows an important adsorption capacity toward MB. This may be assigned firstly to

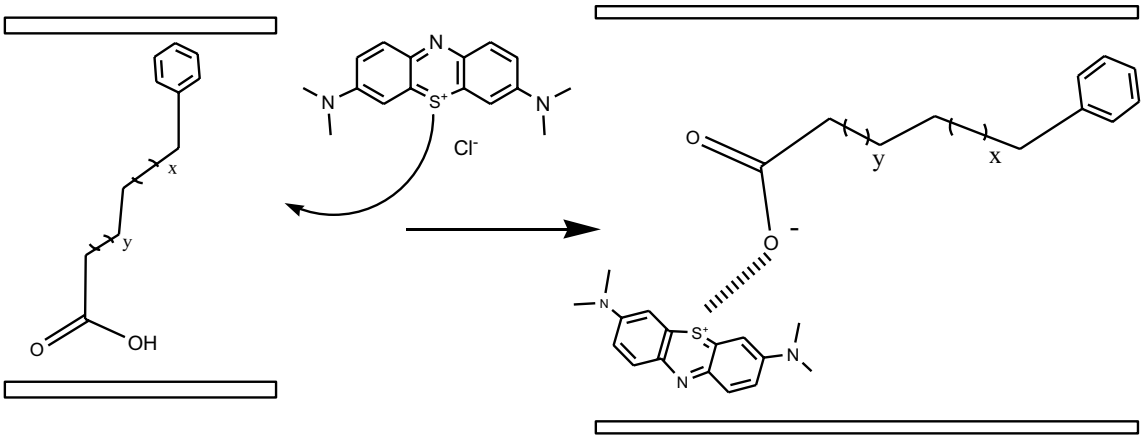

Scheme1 Chemical interaction poly(AA_{25}-*co*-St_{75})/OMMT-MB dye

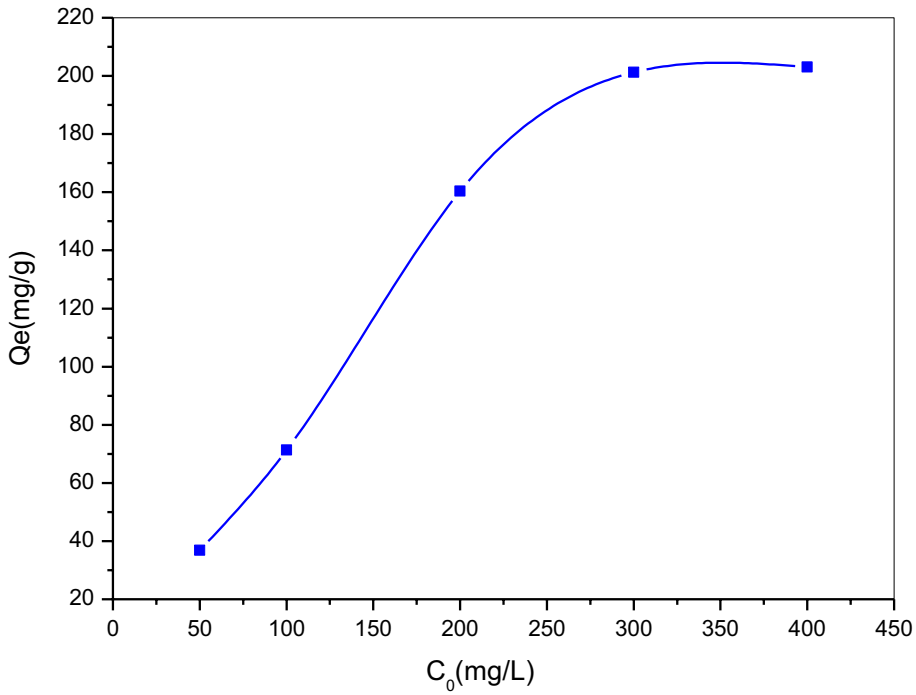

Fig. 10 Dependence of MB adsorption on the initial concentration ($t = 75$ min)

hydrogen bonding formation between the hydroxyl group of the acrylic acid unit and the cationic form of the MB in solution (Scheme 1). Consequently, the dye molecule is diffused in the clay nanoplatelets and it's efficiently removed from the solution. Interestingly, the uptake value of dye is significantly increased by increasing the initial concentration of MB in the solution, achieving an optimal value of 98% for initial concentration of 300 mg g^{-1}, after about 1 h of stirring (Fig. 10). This result confirms the importance of the proposed (nano)composite material for removing efficiently the MB dye from solution.

Conclusion

PAA/OMMT and poly(AA-*co*-St)/OMMT (nano)composites prepared via in situ polymerization, employing an organomodified natural clay, mostly display an intercalated structure. Based on morphological and thermal results, poly(AA-*co*-St)/OMMT (nano)composites was selected as an adsorbent matrix for MB dye. The removal percent of MB by poly(AA_{25}-*co*-St_{75})/OMMT (nano)composite is about 74%. Such complementary study is under investigation regarding the regeneration of the adsorbent material.

References

1. Luecha W, Magaraphan R (2015) Thermal and mechanical properties of nanoclay-poly(acrylic acid) gel reinforced polyethylene terephthalate/clay nanocomposite. e-J Surf Sci Nanotech 13:107–110
2. Yin J, Deng B (2015) Polymer-matrix nanocomposite membranes for water treatment. J Membr Sci 479:256–275
3. Jainesh H, Jhaveri ZV, Murthy P (2016) A comprehensive review on anti-fouling nanocomposite membranes for pressure driven membrane separation processes. Desalination 379:137–154
4. Nasrollahi N, Vatanpour V, Mahmoodi S, Mahmoodi NM (2018) Preparation and characterization of a novel polyethersulfone (PES) ultrafiltration membrane modified with a CuO/ZnO nanocomposite to improve permeability and antifouling properties. Sep Purif Technol 192(2018):369–382
5. Vo VS, Nguyen VH, Mahouche-Chergui S, Carbonnier B, Naili S (2018) Estimation of effective elastic properties of polymer/clay nanocomposites: a parametric study. Compos Part B: Eng 152:139–150
6. Madhumitha G, Fowsiya J, Roopan SM, Thakur VK (2018) Recent advances in starch–clay nanocomposites. Int J Polym Anal Charact 23:331–345
7. Chow WS, Tham WL (2009) Thermal and antistatic properties of polypropylene/organo montmorillonite nanocomposites. Polym Plast Technol Eng 48:342–350
8. Sebastian M, Mathew B (2018) Carbon nanotube-based ion imprinted polymer as electrochemical sensor and sorbent for Zn(II) ion from paint industry wastewater. Int J Polym Anal Charact 23(2018):18–28
9. Nair S, Rajeswari R, Natarajan V (2014) Mukundan concentration-dependent growth and morphology of doped polyaniline nanowires. J Exp Nanosci 9:982–993
10. Yoon SB, Choi BS, Lee KW, Moon JK, Choi YS, Kim JY, Cho H, Kim JH, Kim MS, Yu JS (2014) New mesoporous silica/carbon composites by in situ transformation of silica template in carbon/silica nanocomposite. J Exp Nanosci 9:221–229
11. Lerari D, Peeterbroeck S, Benali S, Benaboura A, Dubois P (2010) Use of a new natural clay to produce poly(methylmethacrylate)-based nanocomposites. Polym Inter 59:71–77
12. Bao Y, Ma J, Yang Z (2011) Preparation and application of poly(methacrylic acid)/montmorillonite nanocomposites. Mater Manuf Process J 26:604–608
13. Khezri K, Haddadi-Asl V, Roghani-Mamaqani H, Salami-Kalajahi M (2012) Synthesis of clay-dispersed poly(styrene-*co*-methyl methacrylate) nanocomposite via miniemulsion atomtransfer radical polymerization: a reverse approach. J Appl Polym Sci 124:2278–2286
14. Jalil A, Khan S, Naeem F, Haider MS, Sarwar S, Riaz A, Ranjha NM (2017) The structural, morphological and thermal properties of grafted pH-sensitive interpenetrating highly porous polymeric composites of sodium alginate/acrylic acid copolymers for controlled delivery of diclofenac potassium. Des Monomers Polym 20:308–324
15. You B, Wen N, Cao Y, Zhou S, Wu L (2009) Preparation and properties of poly[styrene-*co*-(butyl acrylate)-*co*-(acrylic acid)]/silica nanocomposite latex prepared using an acidic silica. Sol Polym Int 58:519–529
16. Kumar S, Jog JP, Natarajan U (2003) Preparation and characterization of poly(methyl methacrylate)–clay nanocomposites via melt intercalation: the effect of organoclay on the structure and thermal properties. J Appl Polym Sci 89:1186–1194
17. Tomasko DL, Han X, Liu DH, Gao W (2003) Supercritical fluid applications in polymer nanocomposites. Curr Opin Solid State Mater Sci 7:407–412
18. Pavlidou S, Papaspyrides CD (2008) A review on polymer-layered silicate nanocomposites. Prog Polym Sci 33:1119–1198
19. Ingram S, Dennis H, Hunter I, Liggat JJ, McAdam C, Pethrick RA (2008) Influence of clay type on exfoliation, cure and physical properties of in situ polymerized poly(methyl methacrylate) nanocomposites. Polym Int 57:1118–1127
20. Lerari D, Benabouraa A (2015) Preparation method effect on thermal properties of PMMA/clay nanocomposite. Mor J Chem 3:202–211
21. Mittal V (2009) Polymer layered silicate nanocomposites: a review. Materials 2:992–1057
22. Xing S, Li R, Si J, Tang P (2016) In situ polymerization of poly(styrene-alt-maleic anhydride)/organic montmorillonite nanocomposites and their ionomers as crystallization nucleating agents for poly(ethylene terephthalate). J Ind Eng Chem 38:167–174
23. Supri AG, Salmah H, Hazwan K (2008) Low density polyethylene-nanoclay composites: the effect of poly(acrylic acid) on mechanical properties, XRD, morphology properties and water absorption. MPJ 3:39–53
24. Zhang B, Li Y, Pan X, Jia X, Wang X (2007) Intercalation of acrylic acid and sodium acrylate into kaolinite and their in situ polymerization. J Phys Chem Sol 68:135–142
25. Liu P, Li L, Zhou NL, Zhang J, Wei SH, Shen J (2006) Synthesis and properties of a poly(acrylic acid)/montmorillonite superabsorbent nanocomposite. J Appl Polym Sci 102:5725–5730
26. Tiwari RR, Natarajan U (2011) Effect of blend composition and organoclay loading on the nanocomposite structure and properties of miscible poly(methyl methacrylate)/poly(styrene-co-acrylonitrile) blends. Polym Eng Sci 51:979–991
27. Tiwari RR, Natarajan U (2012) "Effect of organic modification on the intercalation and the properties of poly(phenylene oxide)/polystyrene blend-clay nanocomposites. J Thermoplast Compos Mater 26:392–415

28. Xing S, Li R, Si J, Tang P (2016) In situ polymerization of poly(styrene-alt-maleic anhydride)/organic montmorillonite nanocomposites and their ionomers as crystallization nucleating agents for poly(ethylene terephthalate). J Ind Eng Chem 38:167–174
29. Siddiqui MN, Redhwi HH, Gkinis K, Achilias DS (2013) Synthesis and characterization of novel nanocomposite materials based on poly(styrene-*co*-butyl methacrylate) copolymers and organomodified clay. Eur Polym J 49:353–365
30. Couvreur L, Charleux B, Guerret O, Magnet S (2003) Direct synthesis of controlled poly(styrene-*co*-acrylic acid)s of various compositions by nitroxide-mediated random copolymerization. Macromol Chem Phys 204:2055–2063
31. Lefay C, Charleux B, Save M, Chassenieux C, Guerret O, Magnet S (2006) Amphiphilic gradient poly(styrene-*co*-acrylic acid) copolymer prepared via nitroxide-mediated solution polymerization. Synthesis, characterization in aqueous solution and evaluation as emulsion polymerization stabilizer. Polymer 47:1935–1945
32. Wei S, Zhang Y, Xu J (2011) Preparation and properties of poly(acrylic acid-*co*-styrene)/Fe_3O_4 Nanocomposites. J Polym Res 18:125–130
33. Kim M, Hwang Y, Ghim HD (2017) Electronically stabilized copoly(styrene-acrylic acid) submicrocapsules prepared by miniemulsion copolymerization. Polymers 9:291
34. El-Sigeny S, Mohamed SK, Abou Taleb MF (2014) Radiation synthesis and characterization of styrene/acrylic acid/organophilic montmorillonite hybrid nanocomposite for sorption of dyes from aqueous solutions. Polym Compos 35:2353–2364
35. Wang L, Zhang J, Wang A (2008) Removal of methylene blue from aqueous solution using chitosan-gpoly(acrylic acid)/montmorillonite superadsorbent nanocomposite. Colloids Surfaces A Physicochem Eng Aspects 322:47–53
36. Bulut Y, Karaer H (2015) Removal of methylene blue from aqueous solution by crosslinked chitosan-g-poly(acrylic acid)/bentonite composite. Chem Eng Commun 36:61–67
37. Lerari D, Peeterbroeck S, Benali S, Benaboura A, Dubois P (2011) Combining atom transfer radical polymerization and melt compounding for producing PMMA/clay nanocomposites. J Appl Polym Sci 121:1355–1364
38. Jada A, Debih H, Khodja M (2006) Montmorillonite surface properties modifications by asphaltenes adsorption. J Petrol Sci Eng 52:305–316
39. Boufatit M, Ait-Amar H, McWhinnie WR (2007) Development of an Algerian material montmorillonite clay. Adsorption of phenol, 2-dichlorophenol and 2,4,6-trichlorophenol from aqueous solutions onto montmorillonite exchanged with transition metal complexes. Desalination 206:394–406
40. Bendaho D, Driss TA, Bassou D (2017) Adsorption of acid dye onto activated algerian clay. Bull Chem Soc Ethiop 31:51–62